TUM/T39–98–17

Nucleon Polarizibilities for Virtual Photons[1]

J. Edelmann, N. Kaiser, G. Piller and W.Weise

Physik-Department, Technische Universität München,
D-85747 Garching, Germany

Abstract

We generalize the sum rules for the nucleon electric plus magnetic polarizability $\Sigma = \alpha + \beta$ and for the nucleon spin-polarizability γ, to virtual photons with $Q^2 > 0$. The dominant low energy cross sections are represented in our calculation by one-pion-loop graphs of relativistic baryon chiral perturbation theory and the $\Delta(1232)$-resonance excitation. For the proton we find good agreement of the calculated $\Sigma_p(Q^2)$ with empirical values obtained from integrating up electroproduction data for $Q^2 < 0.4$ GeV^2. The proton spin-polarizability $\gamma_p(Q^2)$ switches sign around $Q^2 = 0.4$ GeV^2 and it joins smoothly the "partonic" curve, extracted from polarized deep-inelastic scattering, around $Q^2 = 0.7$ GeV^2. For the neutron our predictions of $\Sigma_n(Q^2)$ and $\gamma_n(Q^2)$ agree reasonably well at $Q^2 = 0$ with existing determinations. Upcoming (polarized) electroproduction experiments will be able to test the generalized polarizability sum rules investigated here.

[1]Work supported in part by DFG and BMBF.

1 Introduction

The electromagnetic interaction in the form of real photon absorption and (inelastic) electron scattering is one of the major experimental tools to study the excitation spectrum of the nucleon. It consists of three main components: non-resonant (multi-) meson production near the respective thresholds, excitation of baryon resonances (N^*, Δ etc.) with definite quantum numbers and the parton (quark and gluon) distributions as revealed in deep inelastic lepton scattering.

Unitarity (the optical theorem) and forward dispersion relations connect integrals over the whole nucleon excitation spectrum to certain low energy parameters. Prominent examples are Baldin's sum rule [1] and the Gerasimov-Drell-Hearn sum rule [2]. In the first case the sum of the nucleon electric and magnetic polarizability $\Sigma = \alpha + \beta$ is equated to the integral over the real photon absorption cross section $\sigma_{\rm tot}(\omega)$ weighted by the inverse squared photon lab energy ω,

$$\Sigma = \alpha + \beta = \frac{1}{2\pi^2} \int_{\omega_{th}}^{\infty} \frac{d\omega}{\omega^2} \sigma_{tot}(\omega) \ . \tag{1}$$

Here, $\omega_{th} = m_\pi(1 + m_\pi/2M) = 150$ MeV is the pion photoproduction threshold, and m_π and M denote the pion and nucleon mass, respectively. The resulting value for the proton $\alpha_p + \beta_p = (14.2 \pm 0.3) \cdot 10^{-4}$ fm^3 [3] (recently reevaluated [4] with improved photoproduction data to be $\alpha_p + \beta_p = (13.69 \pm 0.14) \cdot 10^{-4}$ fm^3) is often used in the analysis of low energy proton Compton scattering in order to facilitate the difficult separation of the electric polarizability α_p and magnetic polarizability β_p of the proton. On the theoretical side chiral perturbation theory permits systematic calculations of this quantity [5, 6, 7]. At leading order in the quark mass (or, equivalently, the pion mass) expansion one finds $\alpha_p + \beta_p = 11e^2 g_{\pi N}^2/(768\pi^2 M^2 m_\pi) = 15 \cdot 10^{-4}$ fm^3, a number which is in almost perfect agreement with the empirical determination. However this result does not include the strong paramagnetic effects from the $\Delta(1232)$-resonance. A next-to-leading order calculation leads to $\alpha_p + \beta_p = (14 \pm 4) \cdot 10^{-4}$ fm^3 [7]. At this order one can indeed establish (for the proton) the important cancelation between diamagnetic pion-loop effects ($\sim \ln m_\pi$) and paramagnetic effects from the $\Delta(1232)$-resonance. The theoretical uncertainty (± 4) results from some not very well known low energy parameters entering the calculation and from estimates of the $\Delta(1232)$-contribution itself.

The Gerasimov-Drell-Hearn sum rule [2] connects the squared (proton or neutron) anomalous magnetic moment κ to an integral over the difference of the helicity 1/2 and 3/2 photoabsorption cross sections $\sigma_{1/2,3/2}(\omega)$ weighted by the inverse photon lab energy ω,

$$-\frac{\pi e^2 \kappa^2}{2M^2} = \int_{\omega_{th}}^{\infty} \frac{d\omega}{\omega} \Big[\sigma_{1/2}(\omega) - \sigma_{3/2}(\omega)\Big] \ . \tag{2}$$

At present no direct measurements of these helicity cross sections exist. They have been reconstructed from the single pion photoproduction multipoles [8, 9] and from estimates of the two-pion photoproduction contribution. With this input one finds a qualitative agreement at the 20–30% level between the left and right hand side of eq.(2), but there remains a notorious mismatch in sign once one considers the proton-neutron difference. Upcoming experiments at Mainz (MAMI) and Bonn (ELSA) are devoted to measuring precisely these helicity photoabsorption cross sections $\sigma_{1/2,3/2}(\omega)$ and these measurements will help

to clear up the situation concerning the proton-neutron difference and the validity of the Gerasimov-Drell-Hearn sum rule itself.

From a purely theoretical point of view the Drell-Hearn-Gerasimov sum rule stands or falls with the validity of the no-subtraction hypothesis, since the other ingredients in its derivation, the optical theorem and the Compton low energy theorem, are beyond any doubt. Stated differently the Drell-Hearn-Gerasimov sum rule hinges essentially on the high energy ($\omega \to \infty$) behavior of the (spin-flip) forward Compton amplitude.

On much safer ground is the sum rule for the so-called spin-polarizability γ since it does not require the no-subtraction hypothesis. The nucleon spin polarizability γ is the integral over the difference of the helicity 1/2 and 3/2 photoabsorption cross sections weighted by the inverse third power of the photon lab energy ω,

$$\gamma = \frac{1}{4\pi^2} \int_{\omega_{th}}^{\infty} \frac{d\omega}{\omega^3} \Big[\sigma_{1/2}(\omega) - \sigma_{3/2}(\omega) \Big] \ . \tag{3}$$

Semi-empirical determinations using the pion photoproduction multipoles give $\gamma_p = -1.34 \cdot 10^{-4}$ fm^4 and $\gamma_n = -0.38 \cdot 10^{-4}$ fm^4 [9]. The calculation presented in ref.[6] allows to understand these values in terms of compensative effects from relativistic pion-loops and the $\Delta(1232)$-resonance, $\gamma_p = (2.16 - 3.66) \cdot 10^{-4}$ fm^4 $= -1.50 \cdot 10^{-4}$ fm^4, and $\gamma_n = (3.20 - 3.66) \cdot 10^{-4}$ fm^4 $= -0.46 \cdot 10^{-4}$ fm^4. Obviously the $\Delta(1232)$-effect is dominant in both cases, but the relativistic pion-loop effects are also important in order to reproduce the difference between the proton and neutron value of γ. It should also be mentioned that the calculation of $\gamma_{p,n}$ in ref.[6] is not a complete and systematic order-by-order calculation, but it seems rather convincing that the relativistic pion-loops and the $\Delta(1232)$-resonance account well for the low energy dynamics encoded in $\gamma_{p,n}$ as well as in $\Sigma_{p,n}$.

The purpose of this work is to generalize the Baldin sum rule for $\Sigma = \alpha + \beta$ and the sum rule for γ to virtual photons with $Q^2 > 0$ in the form of energy-weighted integrals over measurable electroproduction cross sections. We will present theoretical predictions for $\Sigma_{p,n}(Q^2)$ and $\gamma_{p,n}(Q^2)$ by evaluating the contributions from the relativistic pion-loop and the $\Delta(1232)$-resonance as done in ref.[6, 10]. In the case of $\Sigma_p(Q^2)$ we can compare with an (approximate) empirical determination using as input electroproduction data from DESY [11]. In the high-Q^2 regime the generalized polarizability sum rules are given by integrals over the (partonic) structure functions $F_1(x)$ and $g_1(x)$ times a characteristic power of $1/Q^2$. We investigate furthermore whether the low energy hadronic side (given in terms pion-loops and the $\Delta(1232)$-resonance) extrapolated upward and the partonic side extrapolated downward match at some intermediate scale. We find that this is indeed the case at $Q^2 \approx 0.5 \ldots 0.7$ GeV^2. This means that the quantities $\Sigma_{p,n}(Q^2)$ and $\gamma_{p,n}(Q^2)$ are not very sensitive to the details of the nucleon excitation spectrum. Our predictions for $\Sigma_{p,n}(Q^2)$ and $\gamma_{p,n}(Q^2)$ can be tested once the relevant electroproduction cross section are available. There exist extended experimental programs to perform such measurements at the electron accelerator laboratories MAMI (Mainz), ELSA (Bonn) and TJNAF (Newport News).

Our paper is organized as follows. In section 2 we present the necessary formalism, the transverse virtual forward Compton amplitude, the optical theorem and the definition of the generalized polarizability sum rules for $\Sigma(Q^2)$ and $\gamma(Q^2)$ in terms of electroproduction cross sections. In section 3 we discuss our results for the proton and the neutron. Section 4 ends with a summary. The appendix includes explicit formulas for the respective virtual

forward Compton amplitudes as they derive from the relativistic one-pion loop graphs of chiral perturbation and $\Delta(1232)$-excitation tree diagrams.

2 Formalism

In this section we present the formalism for transverse virtual forward Compton scattering off the nucleon. The more familiar case of real photon forward Compton scattering can be easily recovered by simply setting $Q^2 = 0$ and will therefore not be treated here separately.

We consider virtual photons with $-q^2 = Q^2 > 0$. The forward transverse amplitude for the process $\gamma^*(q,\epsilon) + N(p) \to \gamma^*(q,\epsilon\,') + N(p)$ reads

$$T = f_1(\omega^2, Q^2)\, \vec{\epsilon}\,'^* \cdot \vec{\epsilon} + f_2(\omega^2, Q^2)\, i\omega\, \vec{\sigma} \cdot (\vec{\epsilon}\,'^* \times \vec{\epsilon}) \ , \tag{4}$$

with $f_{1,2}(\omega^2, Q^2)$ the generalizations of the spin non-flip and spin-flip forward Compton amplitudes, respectively. Crossing symmetry implies that these are even functions of ω. The polarization vectors ϵ and $\epsilon\,'$ satisfy the gauge and transversality conditions $\epsilon \cdot p = \epsilon\,' \cdot p = \epsilon \cdot q = \epsilon\,' \cdot q = 0$. The variable ω is the virtual photon energy in the nucleon rest frame, $\omega = p \cdot q/M$. In terms of the Lorentz-invariant Mandelstam variable $s = (p+q)^2$ one has $\omega = (s - M^2 + Q^2)/2M$.

The Born contributions to $f_{1,2}(\omega^2, Q^2)$ come from the direct and crossed nucleon pole diagram with only a nucleon in the intermediate state. These contributions can be expressed in terms of the (on-shell) electric and magnetic nucleon form factors. At the real photon point $Q^2 = 0$ the Born terms in the limit $\omega \to 0$ agree exactly with the Compton low energy theorems, $f_1(0,0) = -e^2 Z^2/(4\pi M)$, $f_2(0,0) = -e^2\kappa^2/(8\pi M^2)$. Here Z, κ and M denote the electric charge, anomalous magnetic moment and mass of the nucleon (proton or neutron).

We consider here only non-Born contributions to $f_{1,2}(\omega, Q^2)$ which correspond the inelastic electron-nucleon processes. Due to crossing symmetry one can write down the following representation,

$$f_1(\omega^2, Q^2) = \frac{e^2}{4\pi M}\Big[A_1(s, Q^2) + A_1(2M^2 - 2Q^2 - s, Q^2)\Big] \ , \tag{5}$$

$$\omega\, f_2(\omega^2, Q^2) = \frac{e^2}{4\pi M}\Big[A_2(s, Q^2) - A_2(2M^2 - 2Q^2 - s, Q^2)\Big] \ . \tag{6}$$

The dimensionless functions $A_{1,2}(s, Q^2)$ have only a right hand cut starting at the single pion electroproduction threshold $s_{th} = (M + m_\pi)^2$ [10]. In other words, the construction is made such that $A_{1,2}(s, Q^2)$ receive contributions only from all direct (virtual) Compton diagrams and the contributions from all crossed diagrams are generated by the (anti)-symmetrization procedure $s \to 2M^2 - 2Q^2 - s$.

In the physical region of inelastic electron-nucleon scattering ($s > (M + m_\pi)^2$) the optical theorem relates the imaginary parts of $f_{1,2}(\omega^2, Q^2)$ to nucleon structure functions or, equivalently, to inclusive electroproduction cross sections,

$$\mathrm{Im}\, f_1(\omega^2, Q^2) = \frac{e^2}{4M} W_1(\omega, Q^2) = \frac{\omega}{4\pi}\Big(1 - \frac{Q^2}{2M\omega}\Big)\sigma_T(\omega, Q^2) \ , \tag{7}$$

$$\mathrm{Im}\, f_2(\omega^2, Q^2) = \frac{e^2}{4M^2}\Big[G_1(\omega, Q^2) - \frac{Q^2}{M\omega} G_2(\omega, Q^2)\Big]$$

$$= \frac{1}{8\pi}\Big(1-\frac{Q^2}{2M\omega}\Big)\Big[\sigma_{1/2}(\omega,Q^2)-\sigma_{3/2}(\omega,Q^2)\Big] \ . \tag{8}$$

Here $W_1(\omega,Q^2)$ and $G_{1,2}(\omega,Q^2)$ are the usual unpolarized and polarized nucleon structure functions, respectively. $\sigma_T(\omega,Q^2)$ is the transverse electroproduction cross section measured in unpolarized inelastic electron-nucleon scattering. Furthermore, $\sigma_{1/2,3/2}(\omega,Q^2)$ are the helicity cross sections measured with polarized leptons on polarized nucleons with parallel spins pointing either in opposite or in the same direction.

As mentioned in the introduction the combination of a (once-subtracted) forward dispersion relation and the optical theorem leads to the sum rules for the sum of electric and magnetic polarizability $\Sigma = \alpha+\beta$ (Baldin's sum rule), and for the so-called spin-polarizability γ. We now generalize these sum rules, eqs.(1,3), to virtual photons with $Q^2 > 0$ in the (most natural) form,

$$\Sigma(Q^2) = \frac{1}{2\pi^2}\int_{\omega_{th}}^{\infty}\frac{d\omega}{\omega^2}\,\sigma_T(\omega,Q^2) \ , \tag{9}$$

$$\gamma(Q^2) = \frac{1}{4\pi^2}\int_{\omega_{th}}^{\infty}\frac{d\omega}{\omega^3}\,\Big[\sigma_{1/2}(\omega,Q^2)-\sigma_{3/2}(\omega,Q^2)\Big] \ , \tag{10}$$

with $\omega_{th} = m_\pi + (m_\pi^2+Q^2)/2M$ the (single) pion electroproduction threshold. Note that our definition of the generalized polarizabilies $\Sigma(Q^2)$ and $\gamma(Q^2)$ is different from the one in ref.[12]. In this work (non-forward) Compton scattering with a virtual photon in the initial state and a real photon in the final state was considered.

Assuming that the functions $A_{1,2}(s,Q^2)$ introduced in eqs.(5,6) satisfy a (once-subtracted) dispersion relation, which is indeed the case for the relativistic pion-loop diagrams, we arrive after some algebraic manipulation at the following representation of the generalized polarizabilities,

$$\Sigma(Q^2) = \frac{2e^2M}{\pi Q^4}\Big[A_1(M^2,Q^2)-A_1(M^2-Q^2,Q^2)-Q^2A_1'(M^2-Q^2,Q^2)\Big] \ , \tag{11}$$

$$\gamma(Q^2) = \frac{4e^2M^2}{\pi Q^6}\Big[A_2(M^2,Q^2)-A_2(M^2-Q^2,Q^2)-Q^2A_2'(M^2-Q^2,Q^2) - \frac{Q^4}{2}A_2''(M^2-Q^2,Q^2)\Big] \ . \tag{12}$$

Here the prime denotes the partial derivative with respect to the variable s. In order to arrive at the representations eqs.(11,12) it is important that $A_{1,2}(s,Q^2)$ have only right hand cuts, with their discontinuities proportional to the electroproduction cross sections in eqs.(9,10). To make theoretical predictions for $\Sigma(Q^2)$ and $\gamma(Q^2)$ we will compute $A_{1,2}(s,Q^2)$ for the proton and the neutron by evaluating all 52 one-pion loop diagrams of relativistic baryon chiral perturbation theory and the relativistic $\Delta(1232)$-excitation tree-graph (employing the Rarita-Schwinger formalism). These are the dominant processes at low energies where the energy-weighted sum rules eqs.(9,10) for $\Sigma(Q^2)$ and $\gamma(Q^2)$ are almost saturated. The explicit formulas for the various contributions to $A_{1,2}(s,Q^2)$ are given in the appendix.

At large energies and momentum transfer the nucleon structure functions show a scaling behavior, i.e. they depend only on the dimensionless Bjorken variable $x = Q^2/(2M\omega)$. For such kinematics one has $W_1(\omega,Q^2) = F_1(x)$ and $G_1(\omega,Q^2) - (Q^2/M\omega)G_2(\omega,Q^2) =$

$(M/\omega)g_1(x)$, with the unpolarized and polarized nucleon structure functions $F_1(x)$ and $g_1(x)$ in the scaling limit. The contribution of the second spin-dependent structure function $g_2(x)$ is suppressed by a prefactor $-(2xM/Q)^2$. As a consequence of the scaling relations one finds that the large-Q^2 behavior of the generalized polarizabilities $\Sigma(Q^2)$ and $\gamma(Q^2)$ is given by certain integrals over the nucleon structure functions $F_1(x)$ and $g_1(x)$ in the scaling limit times a power of $1/Q^2$,

$$\Sigma(Q^2) = \frac{2e^2M}{\pi Q^4}\int_0^1 dx \frac{x}{1-x}F_1(x) \; , \tag{13}$$

$$\gamma(Q^2) = \frac{4e^2M^2}{\pi Q^6}\int_0^1 dx \frac{x^2}{1-x}g_1(x) \; . \tag{14}$$

The relevant integrals on the right hand side can be evaluated with existing parametrizations [13, 14] of the structure functions $F_1(x)$ and $g_1(x)$. It is interesting to see whether the predictions of our approach valid for small Q^2, which explicitly treats relativistic pion-loops and the $\Delta(1232)$-excitation, matches the QCD-asymptotics valid for large Q^2 at some intermediate scale Q^2.

3 Results and discussion

In this section we present and discuss our results for $\Sigma_{p,n}(Q^2)$ and $\gamma_{p,n}(Q^2)$. The formulas for relativistic pion-loop contributions (given in the appendix) depend on the πN-coupling constant $g_{\pi N}$ for which we use $g_{\pi N} = 13.4$. The evaluation of the relativistic Δ-excitation graphs requires more information. First there is the $\Delta \to N\gamma$ transition strength κ^* for which we use the large-N_c relation to the isovector nucleon magnetic moment, $\kappa^* = 3(1 + \kappa_p - \kappa_n)/2\sqrt{2} = 5.0$. Second, there is the Rarita-Schwinger off-shell parameter Y with the empirical band $-0.8 < Y < 1.7$ [15], for which we choose $Y = 0$. This value is essentially fixed from the $\Delta(1232)$-contribution to $\Sigma(0) = \alpha + \beta$ (see the discussion below). Third, the $\Delta \to N\gamma^*$-transition occurs at non-zero Q^2 and thus there is also a transition form factor $G_\Delta(Q^2)$. We use

$$G_\Delta(Q^2) = \frac{\exp(-0.2Q^2/\mathrm{GeV}^2)}{(1 + 1.41Q^2/\mathrm{GeV}^2)^2} \tag{15}$$

as extracted from pion electroproduction in the $\Delta(1232)$-resonance region in ref.[16]. Apart from the exponential function in the numerator, $G_\Delta(Q^2)$ is the usual dipole fit to the proton electric form factor.

We start the discussion with the values of $\Sigma_{p,n}(Q^2)$ and $\gamma_{p,n}(Q^2)$ at the real photon point $Q^2 = 0$. With the parameter input mentioned before we get

$$\Sigma_p(0) = (5.48 + 8.23) \cdot 10^{-4}\,\mathrm{fm}^3 = 13.71 \cdot 10^{-4}\,\mathrm{fm}^3 \; , \tag{16}$$

$$\Sigma_n(0) = (8.90 + 8.23) \cdot 10^{-4}\,\mathrm{fm}^3 = 17.13 \cdot 10^{-4}\,\mathrm{fm}^3 \; , \tag{17}$$

where the first number in the bracket comes from the pion-loops and the second one from the Δ-excitation. The latter is given by the expression

$$\Sigma_{p,n}^{(\Delta)}(0) = \frac{e^2\kappa_*^2}{18\pi M M_\Delta^2}\left[\frac{M_\Delta^2 + M^2}{M_\Delta^2 - M^2} - 4Y(1+2Y)\right] \; , \tag{18}$$

and its theoretical value $8.23 \cdot 10^{-4}$ fm^3 for $Y = 0$ is about 20% larger than the quasi-empirical value $7 \cdot 10^{-4}$ fm^3 obtained in ref.[17]. Note that the sum of relativistic pion-loops and the Δ-excitation with $Y = 0$ reproduces very well the empirical value for the proton, $\Sigma_p(0) = (13.69 \pm 0.14) \cdot 10^{-4}$ fm^3 [4]. However, the same diagrams overestimate the empirical value for the neutron, $\Sigma_n(0) = (14.40 \pm 0.66) \cdot 10^{-4}$ fm^3 [4] by about 20%. A similar problem was also encountered in the heavy baryon chiral perturbation theory calculation of ref.[7]. It originates from the fact that due to certain numerical coefficients [7] the diamagnetic effects from the pion-loops at next-to-leading order ($\sim \ln m_\pi$) are less strong for the neutron than for the proton.

There is no need to reiterate the values for $\gamma_{p,n}(0)$ given in the introduction and in ref.[6], since $\gamma_{p,n}(0)$ does not depend on the off-shell parameter Y. This feature holds even for the full Q^2-dependent $\gamma_{p,n}(Q^2)$. The reason is that the Y-dependent term in $A^{(\Delta)}_{2,p,n}(s, Q^2)$ (see appendix) is just a quadratic polynomial in s, which makes zero contribution to $\gamma_{p,n}(Q^2)$ according to eq.(12). This independence of the off-shell parameter Y is of course a very welcome feature.

Next, we come to the Q^2-dependent quantities $\Sigma_{p,n}(Q^2)$ as calculated in our approach. They are shown in Fig.1 for the proton and the neutron in the region $0 < Q^2 < 0.4$ GeV^2. The dashed and dotted lines give the relativistic pion-loop and $\Delta(1232)$-contribution, respectively. The full lines correspond to the sum of both contributions. In Fig.2 we show the result of our calculation (full line) together with an evaluation of the sum rule eq.(9) using as input for $\sigma_T(\omega, Q^2)$ the parametrized electroproduction data of ref.[11] (dashed line). Since no transverse-longitudinal separation was done for these electroproduction data one should assign at least a $\pm 15\%$ error band to the dashed line in Fig.2. Note also that the dashed curve obtained from integrating the unpolarized electroproduction data of ref.[11] does not exactly extrapolate the value $\Sigma_p(0) = 13.7 \cdot 10^{-4}$ fm^3 at the real photon point $Q^2 = 0$. Within the uncertainty of the empirical $\Sigma_p(Q^2)$ (obtained from integrating the electroproduction data) there is good agreement with our calculation. Note that the Q^2-dependence of the pion-loops is entirely due to the pion and nucleon propagators in the loop-diagrams, and the Q^2-dependence of the $\Delta(1232)$-contribution is essentially due to the phenomenological $\Delta \to N\gamma^*$ transition form factor $G_\Delta(Q^2)$ given in eq.(15). In Fig.3 we show the results for $\Sigma_{p,n}(Q^2)$ of our calculation (full lines) together with the partonic prediction eq.(13) extrapolated downward to $Q^2 = 0.5$ GeV^2. The integrals $\int_0^1 dx\, 2xF_1(x)/(1-x)$ were evaluated with parametrized parton distributions of ref.[13] taken at $Q^2 = 1$ GeV^2. The resulting values of these integrals are 0.453 for the proton and 0.313 for the neutron. It is interesting to observe that the low Q^2-behavior given by the pion-loops and the $\Delta(1232)$-resonance matches approximately with the downward extrapolated partonic curve at $Q^2 = 0.5$ GeV^2. The integrated quantities $\Sigma_{p,n}(Q^2)$ are obviously not very sensitive to details of the nucleon excitation spectrum.

Fig.4 shows the Q^2-dependent spin-polarizabilities $\gamma_{p,n}(Q^2)$ for the proton and the neutron in the region $0 < Q^2 < 0.6$ GeV^2. For these quantities a strong cancelation between (positive) pion-loop contributions and (negative) $\Delta(1232)$-contributions is taking place. For very small Q^2 the $\Delta(1232)$-effects are actually dominant as witnessed by the negative values at the real photon point $Q^2 = 0$. Note that the $\Delta(1232)$-contribution decreases faster in magnitude (due to the transition form factor $G_\Delta(Q^2)$) than the pion-loop contribution. As a consequence $\gamma_{p,n}(Q^2)$ pass through zero around $Q^2 \simeq 0.4$ GeV^2. At present there are not

enough data for the helicity cross sections $\sigma_{1/2,3/2}(\omega, Q^2)$ such that one could integrate them up to get an empirical determination of $\gamma_{p,n}(Q^2)$. However these will be measured in the near future at the electron accelerator laboratories MAMI, ELSA and TJNAF. In particular one can then test our result for the transition through zero of $\gamma_{p,n}(Q^2)$ at $Q^2 \simeq 0.4$ GeV^2. Of course, the one-loop chiral perturbation theory treatment of the pion-cloud contribution is likely to become uncertain at $Q^2 > 0.5$ GeV^2. Effects beyond one-loop, such as form factors of the interacting $\gamma^* \pi N$ system, can make these contributions softer so that the zero of $\gamma_{p,n}(Q^2)$ may be shifted to somewhat smaller values of Q^2.

Finally, we show in Fig.5 the results of our calculation for $\gamma_{p,n}(Q^2)$ (full lines) together with the partonic prediction (dashed lines) extrapolated downward. The integrals $\int_0^1 dx x^2 g_1(x)/(1-x)$ were evaluated with the parton distributions of ref.[14] taken at $Q^2 = 1$ GeV^2. The resulting values for these integrals are $2.72 \cdot 10^{-2}$ for the proton and $-1.52 \cdot 10^{-3}$ for the neutron. Again one observes a smooth transition from the hadronic side (pion-loops plus $\Delta(1232)$) to the partonic side around $Q^2 = (0.6 - 0.7)$ GeV^2 in the case of the proton. The partonic prediction for $\gamma_n(Q^2)$ is very small and negative, whereas the sum of pion-loop and $\Delta(1232)$-contributions is positive in the low-Q^2 region. There is an almost complete cancelation of the pion-loop and $\Delta(1232)$-contributions at $Q^2 = 0.5$ GeV^2, and this zero would move upward with a slight change of the transition form factor $G_\Delta(Q^2)$. Within the accuracy of our approach one can say that there is no mismatch for the neutron's $\gamma_n(Q^2)$ between the hadronic prediction at low Q^2 and the partonic prediction extrapolated downward.

4 Summary

In this work we have generalized the sum rules for the nucleon electric plus magnetic polarizabilities, $\Sigma = \alpha + \beta$, and the so-called spin-polarizability γ to virtual photons with $Q^2 > 0$. Once the respective unpolarized and polarized nucleon electroproduction cross sections $\sigma_T(\omega, Q^2)$ and $\sigma_{1/2,3/2}(\omega, Q^2)$ are measured these sum rules can be evaluated empirically. We have presented a calculation of the quantities $\Sigma_{p,n}(Q^2)$ and $\gamma_{p,n}(Q^2)$ at low Q^2 in terms of relativistic pion-loop graphs of chiral perturbation theory and the $\Delta(1232)$-excitation. The off-shell parameter of the $\Delta N \gamma$-vertex ($Y = 0$) was fixed through the value $\Sigma_p(0) = 13.7 \cdot 10^{-4}$ fm^3, and we used a phenomenological $\Delta \to N \gamma^*$ transition form factor $G_\Delta(Q^2)$ extracted from pion electroproduction in the Δ-resonance region. In the case of the proton's $\Sigma_p(Q^2)$ we could compare with experimental values and found good agreement within the accuracy of the data. The spin polarizabilities $\gamma_{p,n}(Q^2)$ pass through zero (starting from negative values) at $Q^2 = 0.4 \ldots 0.5$ GeV^2 as a result of the cancelation between pion-loop and $\Delta(1232)$-effects. Furthermore, we found that there is a smooth transition from the hadronic side to the partonic side at $Q^2 = 0.5 \ldots 0.7$ GeV^2 for both $\Sigma_{p,n}(Q^2)$ and $\gamma_{p,n}(Q^2)$. It means that these quantities are not very sensitive to details of the nucleon excitation spectrum.

Appendix

Here we collect explicit formulas for the functions $A_1(s,Q^2)$ and $A_2(s,Q^2)$. The 52 one-pion loop diagrams evaluated in relativistic chiral perturbation theory give rise to the following contributions for the proton,

$$\begin{aligned}
A_{2,p}(s,Q^2) &= g_{\pi N}^2\Big\{ -\underline{J}_0(s)+\frac{3}{2}\underline{J}_1(s)+4\underline{\gamma}_3(s,Q^2)-2\underline{\Gamma}_3(s,Q^2)+\frac{1}{2}(3M^2-Q^2-s)\Gamma_2(s,Q^2) \\
&\quad +(s-M^2+Q^2)\Big[\Gamma_1(s,Q^2)-\frac{Q^2}{2}G_4(s,Q^2)+\frac{M^2}{2}G_6(s,Q^2)\Big]+Q^2\Big[\Gamma_5(s,Q^2) \\
&\quad -2M^2G_5(s,Q^2)\Big]+\frac{Q^2}{s-M^2}\Big[\frac{3}{2}\underline{J}_1(s)+4\underline{\gamma}_3(s,Q^2)+2\underline{\Gamma}_3(s,Q^2)+M^2\underline{\Gamma}_6(s,Q^2) \\
&\quad +Q^2\Big(\underline{\Gamma}_5(s,Q^2)-\underline{\Gamma}_4(s,Q^2)\Big)\Big]+\frac{3Q^2M^2}{(s-M^2)^2}\Big[\underline{\underline{J}}_1(s)-\underline{\underline{J}}_0(s)\Big]\Big\}\ , \qquad (19) \\
A_{1,p}(s,Q^2) &= A_{2,p}(s,Q^2)+g_{\pi N}^2\Big\{(M^2-Q^2+m_\pi^2-s)[\Gamma_1(s,Q^2)-\Gamma_2(s,Q^2)] \\
&\quad +2\underline{\Gamma}_3(s,Q^2)-4\underline{\gamma}_3(s,Q^2)+2m_\pi^2[\gamma_2(s,Q^2)-\gamma_1(s,Q^2)-\gamma_0(s,Q^2)]\Big\}\ , \qquad (20)
\end{aligned}$$

and the neutron,

$$\begin{aligned}
A_{2,n}(s,Q^2) &= g_{\pi N}^2\Big\{4\underline{\gamma}_3(s,Q^2)+4\underline{\Gamma}_3(s,Q^2)+(3M^2-Q^2-s)\Gamma_2(s,Q^2)-4M^2Q^2G_5(s,Q^2) \\
&\quad +(s-M^2+Q^2)[2\Gamma_1(s,Q^2)-Q^2G_4(s,Q^2)+M^2G_6(s,Q^2)]\Big\}\ , \qquad (21) \\
A_{1,n}(s,Q^2) &= A_{2,n}(s,Q^2)+g_{\pi N}^2\Big\{2(M^2-Q^2+m_\pi^2-s)[\Gamma_1(s,Q^2)-\Gamma_2(s,Q^2)] \\
&\quad +\frac{8m_\pi^2}{s-M^2+Q^2}\Big[\underline{\gamma}_3(s,Q^2)-\underline{\gamma}_3(M^2-Q^2,Q^2)+\underline{\Gamma}_3(s,Q^2)-\underline{\Gamma}_3(M^2-Q^2,Q^2)\Big] \\
&\quad -4\underline{\Gamma}_3(s,Q^2)-4\underline{\gamma}_3(s,Q^2)+2m_\pi^2[\gamma_2(s,Q^2)-\gamma_1(s,Q^2)-\gamma_0(s,Q^2)]\Big\}\ . \qquad (22)
\end{aligned}$$

The various loop functions are generalizations of the ones defined for $Q^2=0$ in ref.[5] to virtual photons with $Q^2>0$ using $h_\gamma(x,y;s,Q^2)=m_\pi^2(1-y)+M^2y^2+(s-M^2)xy(y-1)+Q^2x(1-x)(1-y)^2$ in their Feynman parameter representation. The underbar on a loop function means subtraction at $s=M^2$, e.g. $\underline{\gamma}_3(s,Q^2)=\gamma_3(s,Q^2)-\gamma_3(M^2,Q^2)$. Similarly, the double underbar means two subtractions at $s=M^2$, e.g. $\underline{\underline{J}}_0(s)=\underline{J}_0(s)-(s-M^2)\underline{J}_0'(M^2)$.

The tree diagrams with $\Delta(1232)$-resonance excitation when evaluated relativistically using a Rarita-Schwinger spinor for the spin-3/2 field give an equal contribution for the proton and the neutron,

$$\begin{aligned}
A_2(s,Q^2) &= \frac{\kappa^{*2}G_\Delta^2(Q^2)}{72M^2M_\Delta^2}\Big\{\frac{1}{s-M_\Delta^2}\Big[(s-M^2)^2(3M_\Delta^2-M^2)+Q^2(sM^2-3M^4 \\
&\quad -3M^2Q^2+3M^2M_\Delta^2+4sM_\Delta M-sQ^2+3sM_\Delta^2-Q^4)\Big]-2(4Y+1)Q^2 \\
&\quad \cdot(M^2+s+Q^2)-(4Y+1)^2[Q^2(s+M^2+4M_\Delta M)+(s-M^2)^2]\Big\}\ , \qquad (23) \\
A_1(s,Q^2) &= A_2(s,Q^2)-\frac{\kappa^{*2}G_\Delta^2(Q^2)}{12M^2(s-M_\Delta^2)}\Big\{Q^2(s+M^2+2M_\Delta M)+(s-M^2)^2\Big\}\ . \qquad (24)
\end{aligned}$$

References

[1] A.M. Baldin, *Nucl. Phys.* **18** (1960) 310; L.I. Lapidus, Sov. Phys. JEPT **16** (1963) 964.

[2] S.B. Gerasimov, *Sov. J. Nucl. Phys.* **2** (1966) 430; S.D. Drell and A.C. Hearn. *Phys. Rev. Lett.* **16** (1966) 908.

[3] M. Damashek and F.J. Gilman, *Phys. Rev.* **D1** (1970) 1319.

[4] D. Babusci, G. Giordano and G. Matone, *Phys. Rev.* **C57** (1998) 291

[5] V. Bernard, N. Kaiser and U.-G. Meißner, *Nucl. Phys.* **B373** (1992) 346.

[6] V. Bernard, N. Kaiser, J. Kambor and U.-G. Meißner, *Nucl. Phys.* **B388** (1992) 315.

[7] V. Bernard, N. Kaiser, U.-G. Meißner and A. Schmidt, *Phys. Lett.* **B319** (1993) 269; *Z. Phys.* **A348** (1994) 317.

[8] I. Karliner, *Phys. Rev.* **D7** (1973) 2717; R.L. Workman and R.A. Arndt, *Phys. Rev.* **D45** (1992) 1789.

[9] A.M. Sanforfi, C.S. Whisnant and M. Khandaker, *Phys. Rev.* **D** 50 (1994) 6681.

[10] V. Bernard, N. Kaiser and U.-G. Meißner, *Phys. Rev.* **D48** (1993) 3062.

[11] F.W. Brasse *et al.*, *Nucl. Phys.* **B110** (1976) 413.

[12] D. Drechsel, G. Knöchlein, A. Metz and S. Scherer, *Phys. Rev.* **C55** (1997) 424; T.R. Hemmert, B.R. Holstein, G. Knöchlein, and S. Scherer, *Phys. Rev.* **D55** (1997) 2630; *Phys. Rev. Lett.* **79** (1997) 22.

[13] A.D. Martin, R.G. Roberts and W.J. Stirling, *Phys. Rev.* **D51** (1995) 4756.

[14] T. Gehrmann and W.J. Stirling, *Phys. Rev.* **D53** (1996) 6100.

[15] M. Benmerrouche, R.M. Davidson and N.C. Mukhodpadhyay, *Phys. Rev.* **C39** (1989) 2339.

[16] V. Burkert and Z. Li, *Phys. Rev.* **D47** (1993) 46; S. Galster *et al.*, *Phys. Rev.* **D5** (1972) 519; W. Bartel *et al.*, *Phys. Lett.* **B28** (1968) 148.

[17] N.C. Mukhodpadhyay, A.M. Nathan and L. Zhang, *Phys. Rev.* **D47** (1993) R7.

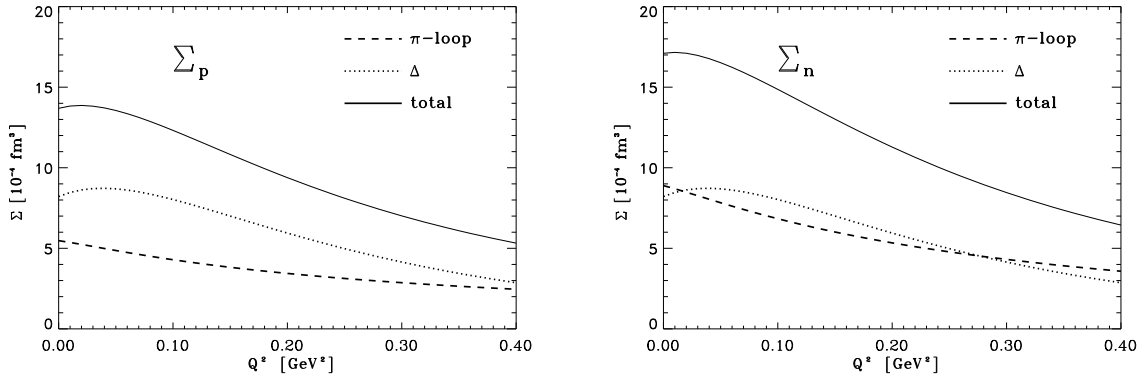

Fig.1: The sums of electric and magnetic polarizabilities $\Sigma_{p,n}(Q^2)$ for the proton and the neutron as a function of Q^2. The dashed, dotted and full lines are explained in the figure.

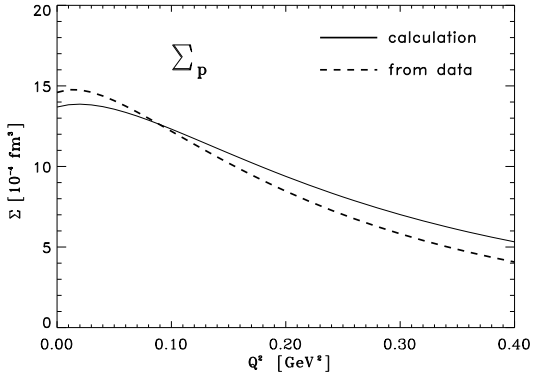

Fig.2: The calculated quantity $\Sigma_p(Q^2)$ (full line) compared to an empirical determination using the electroproduction cross sections of ref.[11] (dashed line).

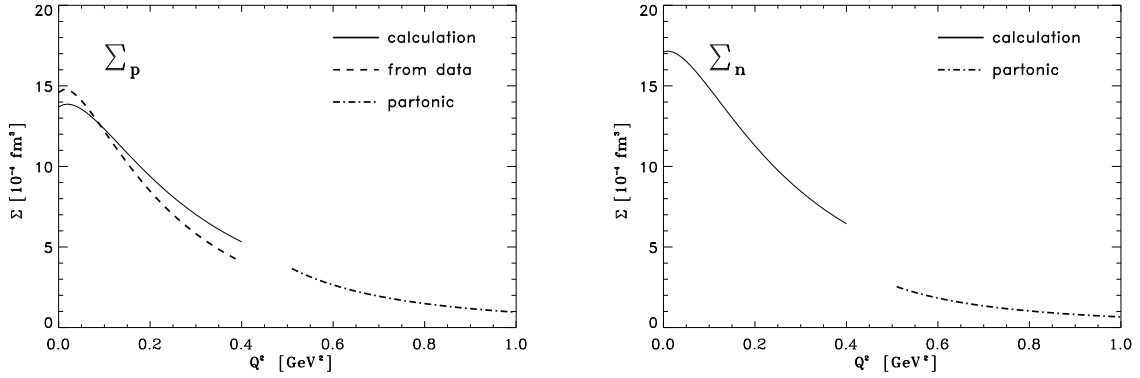

Fig.3: $\Sigma_{p,n}(Q^2)$ for the proton and the neutron as a function of Q^2. The prediction at small Q^2 (full lines) is due to relativistic pion loops and the $\Delta(1232)$-resonance. The dashed-dotted lines result from extrapolating downward the partonic prediction.

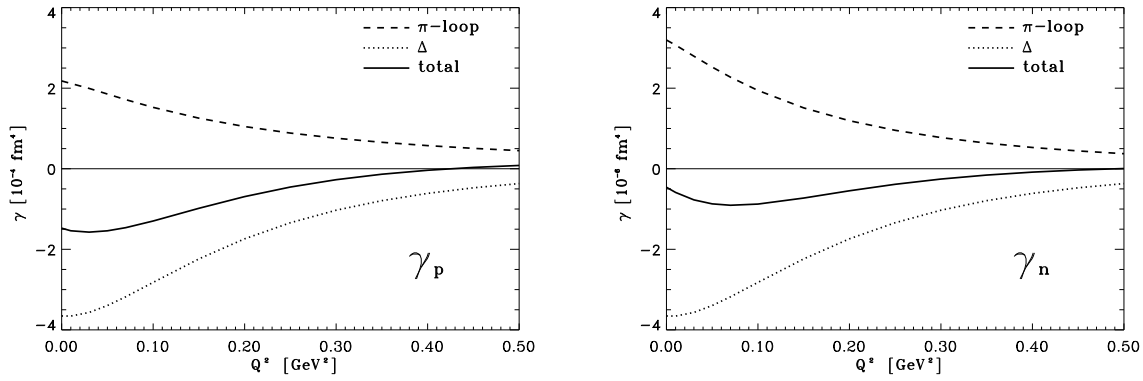

Fig.4: The generalized spin polarizabilities $\gamma_{p,n}(Q^2)$ for the proton and the neutron as a function of Q^2. The dashed, dotted and full lines are explained in the figure.

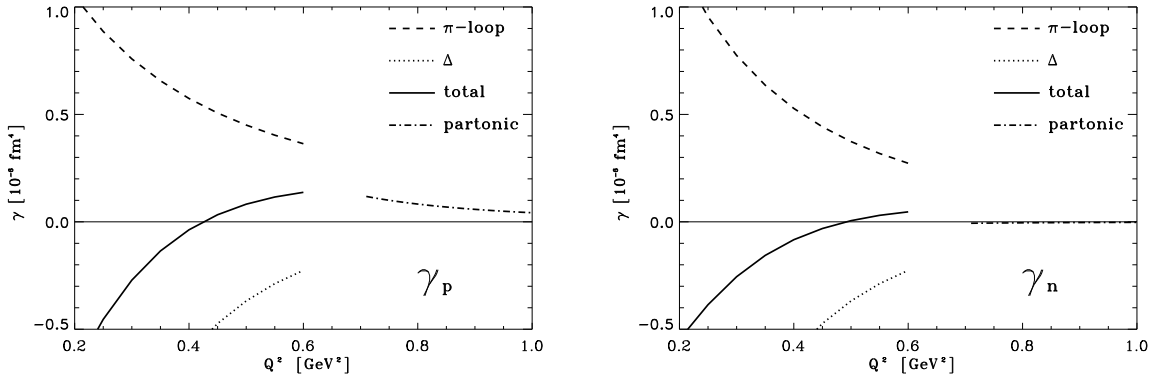

Fig.5: $\gamma_{p,n}(Q^2)$ for the proton and the neutron as a function of Q^2. The prediction at small Q^2 (full lines) is due to relativistic pion loops and the $\Delta(1232)$-resonance. The dashed-dotted lines result from extrapolating downward the partonic prediction.